Cite this paper as:
Ngo N.T., Indraratna B., Rujikiatkamjorn C. (2018) Load-Deformation Responses of Ballasted Rail Tracks: Laboratory and Discrete-Continuum Modelling. In: Shi X., Liu Z., Liu J. (eds) Proceedings of GeoShanghai 2018 International Conference: Transportation Geotechnics and Pavement Engineering. GSIC 2018, pp: 189-198, Springer, Singapore

Load-deformation Responses of Ballasted Rail Tracks: Laboratory and Discrete–Continuum Modelling

Trung Ngoc Ngo[1], Buddhima Indraratna[2] and Cholachat Rujikiatkamjorn[3]

[1,2,3] Centre for Geomechanics and Railway Engineering (CGRE) and ARC Training Centre for Advanced Technologies in Rail Track Infrastructure (ITTC-Rail), University of Wollongong, NSW 2522, Australia.
trung@uow.edu.au

Abstract. The fast urbanization and frequent traffic congestion of roads have led to increasing attention being focused on ballasted tracks for heavy haul and passenger transport. The complex mechanism of the degradation and deformation of ballast and the urgent request for effective track operation that requires a better understanding of the load-deformation responses of ballast to improve the existing conventional railroad design for future high speed trains and heavy hauls. In this study, the load-deformation responses of ballast under cyclic loads is measured in the laboratory using a novel large-scale Track Process Simulation Apparatus (TPSA). A novel coupling model built on discrete element method (DEM) and finite element method (FEM) is developed to predict the load-deformation responses of a ballasted track capturing the interaction of discrete ballast grains and continuum subgrade. In this coupling approach, the discrete nature of ballast particles are modelled by DEM and the subgrade media is modelled as continuum elements by FEM. The results indicate that significant settlements are observed at the beginning of loading stage, followed by increased deformation, arriving at a constant value towards the end of tests. Contact force distributions, stress contours and corresponding broken bonds are captured.

Keywords: Railway Ballast, Cyclic Loading, Coupled Discrete-Continuum Modelling.

1 Introduction

Australia plays a leading role in the development of heavy freight trains that include 3–5 km long trains with axle loads exceeding 30 tonnes to optimise the efficiency of transport the mining and agricultural sectors [1]. Ballast is an essential component of the rail track substructure, and it is commonly used to: (a) distribute the applied train loading to the underlying subgrade, (b) maintain track alignment, and (c) provide track drainage [2, 3]. Upon repeated train loads, the sharp corners of ballast aggregates break; this causes differential track settlement [4]. In addition, the ballast layer can be fouled by upward migration of subgrade clay fines and the downward migration of coal spilling from wagons [5-8], all of which seriously affect the drainage capacity of the track. It is noted that the ballast often has minimum lateral support in the field, the lateral confining pressure therefore should be increased to improve lateral stability [9]. The performance of ballast is affected by the overall characteristics of a granular mass such as the particle size distribution, the void ratio, and the relative density [10, 11]. While the properties of individual particles of ballast such as size, shape, and angularity govern its degradation under traffic loading, deformation is also influenced by the magnitude of wheel (or axle) load, the number of load cycles, frequency (equivalent to train speed), and the impact loads [12, 13]. The magnitude of the impact loads depends on the type and nature of surface imperfections on the wheels and rails, as well as on the track's dynamic response.

In conventional track design, the ballast is often considered as an elastic medium where its degradation and associated plastic deformation is ignored. This issue is due to not understanding the complexity of particle degradation and fouling problems and not having a proper constitutive model. The constitutive behavior of granular materials has been studied by various researchers using the discrete element modeling approach [14-16]. This approach to model the track granular media is promising as it can handle particles at micro-scale. In the last decades, the use of planar geosynthetic products such as geogrid, geotextile or geocomposite (bonding geogrid with geotextile) has been more popular as they are economical and increase track stability. Previous researches have indicated that geogrid reinforcement reduces the settlement and degradation of ballast [17-19] attributed to the interlocking effect that restricts the lateral movement of ballast. In addition, recent studies have shown that a geocell (three dimensional, polymeric cells, interconnected at the joint) can provide much better lateral track confinement than planar reinforcement [20].

Continuum approaches have been widely used to model granular material assemblies, and various conventional continuum constitutive models have been introduced to capture their stress-strain responses of granular materials. It is noted that due to the discrete nature of ballast particles, the continuum approach could not accurately simulate their micro-mechanical behavior governed by the fabric anisotropy, contact orientations and strain localisations. Meanwhile the discrete element method (DEM) has been increasingly used in the recent past as an alternative to the continuum-based methods for the study of granular materials. This paper presents a coupled DEM-FEM modelling approach to takes advantage of each numerical scheme to provide a realistic solution to model an integrated and layered ballasted track. The model is validated by extensive large-scale tests and presented in the following sections.

2 Experimental Investigations

A large-scale Track Process Simulation Apparatus (TPSA) can simulate a ballast assembly of: 800 mm × 600 mm × 600 mm was used to measure the deformation and degradation of ballast under cyclic loads, as shown Figure 1. Ballast was selected from Bombo quarry, New South Wales, Australia, then cleaned and sieved following to the Australia Standards [21]. The particle size distribution of the ballast had an average particle size d_{50}=38 mm, which is similar to current Australian practices. To simulate actual field conditions, a 150 mm-thick sub-ballast and subgrade layer, made from coarse sand and gravel mixture (unit weight of 18.5 kN/m3), was placed at the bottom of the TPSA. The ballast was then filled above the sub-ballast and compacted in every 50 mm-thick sub-layer to a unit weight of 15.3 kN/m3, until a total height of the ballast layer achieved 300 mm. A lateral confining pressure of σ_{xx}=10 kPa was applied in the direction parallel to sleepers to simulate low confinement given by the shoulder ballast in the field [22]. A cyclic load was applied via dynamic actuator with a maximum induced cyclic stress of σ_{yy}=420 kPa, the frequency of f=15 Hz, simulating a freight train (i.e. axle load: 30 tonnes; speed: 90 km/h). All tests were conducted up to 500,000 load cycles. The detailed experimental program and analysis of these tests were presented elsewhere by Indraratna et al. [3] and they concluded that the ballast showed a significant deformation within the first 100,000 load cycles, followed by a decreased rate of settlement up to 300,000 cycles, and then kept almost unchanged toward the end of tests. Ballast breakage was quantified after the completion of every test by comparing the differences of ballast particle size distribution curves before and after every test, using the ballast breakage index (BBI) proposed earlier by Indraratna et al [23]. Some of the results of these tests are re-used in this study to calibrate and validate the combined DEM-FEM model.

3 Discrete–Continuum Modelling Approach

3.1 Discrete Element Method

The discrete element method (DEM) introduced by Cundall and Strack [24] has been increasingly applied to study the micromechanical behavior of granular materials [25-28]. In DEM, particles are treated as rigid bodies and have a negligible contact area (i.e. at a point). A soft contact approach is commonly used at the contacts allowing the rigid particles to overlap one another at contact points and the extent of the overlap is related to the magnitude of contact forces governed by the force-displacement law. The force-displacement law derives the contact force acting on two entities in contact to the relative displacement between them. In DEM, particles are spherical in three-dimension or

circular in two-dimension; however it is also possible to create particles of arbitrary shape by connecting more spheres together at appropriate sizes and positions (i.e. clumps). Each clump composes of a number of overlapping spheres and acts as a rigid entity with a deformable boundary [29]. Furthermore, it is possible to bond particle together and model fracture of rock mass or breakage of granular materials when the bonds break, which was used by Indraratna et al. [3] to capture ballast breakage. Irregularly-shaped ballast particles were simulated in DEM by connecting of specified numbers of circular balls together to represent appropriate angularity and sizes. In the current DEM analysis, the material properties of the coupled DEM-FEM numerical model are given in Table 1. These values were determined based on the calibration with laboratory test data.

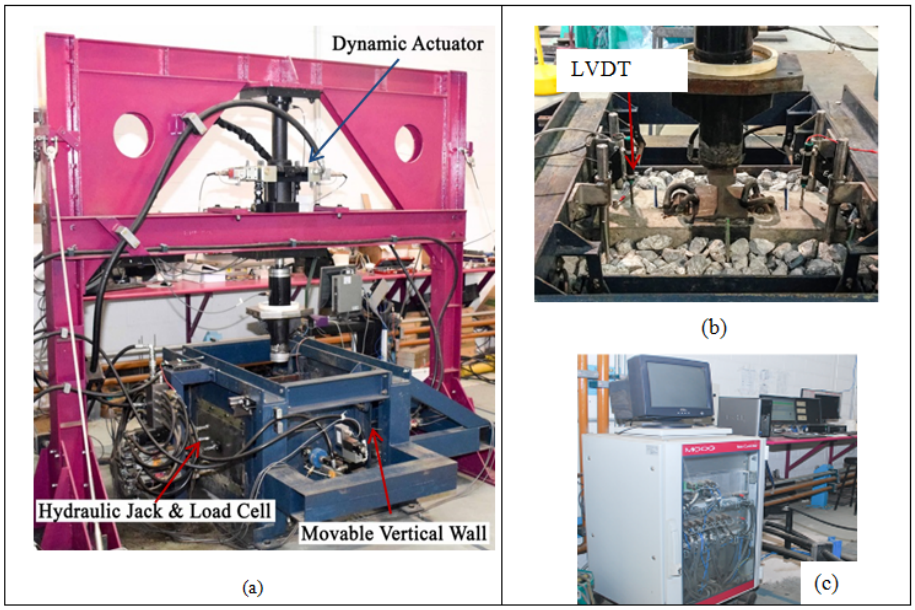

Fig.1. (a) Track Process Simulation Apparatus –TPSA; (b) Ballast assembly; (c) Data logger instrumentations

Table 1. Micromechanical parameters of ballast particles and walls used in DEM simulation.

Micro-mechanical parameters	Values
Radius of particle (m)	1.8 × 10-3 - 16 × 10-3
Inter-particle coefficient of friction	0.80
Particle normal and shear contact stiffness (N/m)	3.58×10^8
Normal and shear stiffness of wall (N/m)	3×10^7
Parallel bond normal and shear stiffness (N/m)	6.25×10^{10}
Parallel bond normal and shear strength (N/m^2)	5.78×10^6
Parallel bond radius multiplier	0.5
Particle unit weight (kN/m^3)	15.3

3.2 Continuum Modelling Approach

The subgrade and sub-ballast were simulated as a homogeneous layer having 150 mm depth, as shown in Figure 2. Given the symmetry of the tracks, the left and right boundaries of the subgrade model were prevented from lateral movements while they allowed displacing vertically. The boundaries were considered as absorbent (viscous) to avoid spurious reflection of the cyclic wave. The bottom boundary was modelled as a pinned support (i.e. both the lateral and vertical displacements were restrained). The subgrade and sub-ballast were represented with a standard elasto-plastic Mohr Coulomb model where the model parameters (i.e. Young's modulus E, Poison's ratio ν, cohesion c, friction angle ϕ, and dilatancy angle ψ) were determined from tests carried out on the subgrade soil. In the current

coupled analysis, the subgrade having E =45 MPa, $\nu = 0.32$, $c = 17$ kPa, $\phi = 14^0$, and $\psi = 4^0$ were used. It is noted that the DEM and FEM share the same geometrical boundaries where they are interfaced. Initially, a series of walls is generated in the DEM zone, where each wall at the interface corresponding to a single surface segment (continuum element) of the FEM zone [30].

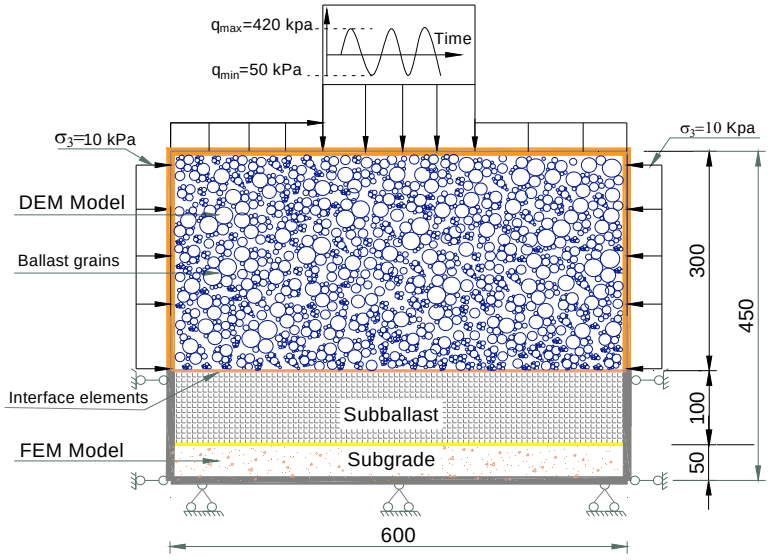

Fig. 2. Schematic diagram of a coupled DEM-FEM model (after Ngo et al. [22])

3.3 Coupled Discrete – Continuum Analysis

A coupled DEM-FEM that combines the discrete and continuum modelling approaches through the development of a force-displacement transmission mechanism at the ballast-subgrade interface is illustrated in Fig.2; and the model dimensions represent the large-scale TPSA. Given that the movement of ballast in the longitudinal direction (along with the direction of train passage) is very small due to the confinement provided by embedded sleepers, the current analysis is carried out in an equivalent plane strain condition that is usually representative of long and straight tracks [31]. A ballast layer was modelled using the DEM, whereas subgrade layer was modelled by continuum approach. The interaction between ballast layer and sub-ballast was achieved through interface elements at the DEM and FEM boundary. Principally, the coupling between the DEM and FEM is initiated at the ballast-sub-ballast interfaces by: (i) applying contact forces acting on the discrete particles at the interface as applied forces at the boundary of the continuum grids, and (ii) treating the nodal displacements as velocity boundary conditions for the discrete particles (i.e. apply velocity to the particles). Subject to loading, the DEM zone (continuum mesh) deform in large strain; the displacements are transferred back to DEM, so that the walls in DEM zone moves in exactly the same way as the boundary segments of the FEM grid. The resulting contact forces at walls (i.e. due to particles contacting to the walls) are then transferred to FEM as applied grid-point forces. A detailed mathematical framework to assist the coupled model in transferring the forces and displacements between the two domains is presented earlier by Ngo et al [22].

4 Results and Discussion

4.1 Load-deformation Responses

Figure 3 shows the applied cyclic stress versus accumulated axial strain measured from the coupled DEM-FEM analysis at different loading cycles. It is noted that the axial strains were determined excluding any settlements of capping and subgrade layers. It is observed that the predicted axial strains increase considerably in the first 1000 load cycles (i.e. up to around 3% axial strain), came after by gradually increasing axial strains in the next 5,000 cycles, and then kept relatively unchanged towards the end (10,000 cycles). These observations are in good agreement with those

measured in the experiment. Indeed, the area confines by the cyclic (hysteresis) loops becomes increasingly smaller as the number of cycles increases, indicating that the ballast aggregates through cyclic densification begin to respond more elastically with time. The hysteresis loops are also very similar to those measured in laboratory experiments [3]. This indicates that the ballast sample experiences significant re-arrangement and densification upon initially applied load cycles, but after achieving a threshold compression, any further loading will resist further deformation and promote particles crushing. This finding is in agreement with results presented by Lobo-Guerrero and Vallejo[32] where they observed that the ballast deformation considerably increased when the particle breakage was considered analysis.

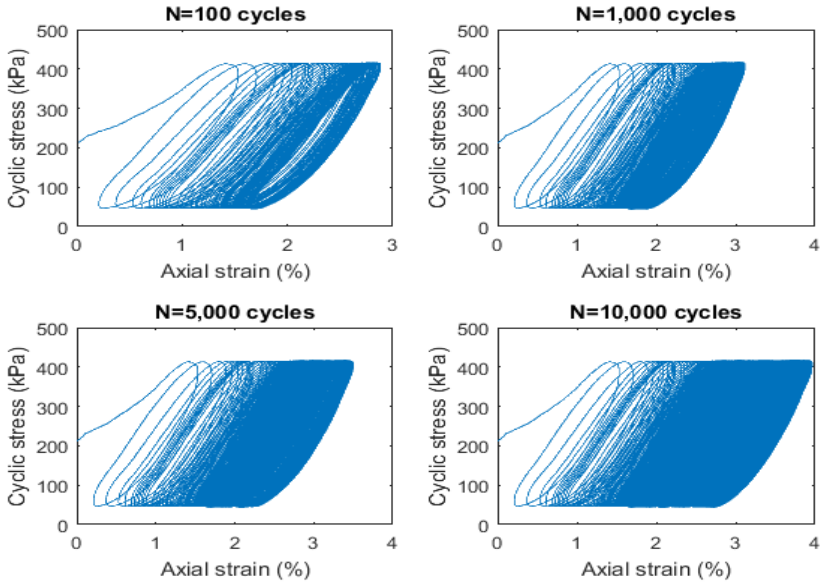

Fig. 3. Applied cyclic stress versus axial strain at different numbers of load cycles.

Applied loads transmit to the discrete ballast particles in the form of contact force-chains, where the pattern of force-fabric varies with the packing structure [33]. Figure 4 presents the inter-particle contact forces of the ballast specimens together with vertical stress contours at N=10, 1000 and N=5000 load cycles. Each contact force is represented at the contact point oriented in the direction of the force and with a thickness proportional to its intensity. It is seen that the majority of contact forces arrange vertically. Subjected to cyclic loads, there is a concentration of large contact forces occurring beneath the loading plate, and around wall edges, while a significant part of the applied load is still vertically transmitted to the underlying sub-ballast (capping) and subgrade (Fig. 4b-c). It is also noted that the force distribution in the DEM region is always heterogeneous, where the maximum contact forces vary with load cycles. The compressive stress (σ_{yy}) in the subgrade is greater mainly around the interface area that is directly in contact with the aggregates, and decreases with depth as expected.

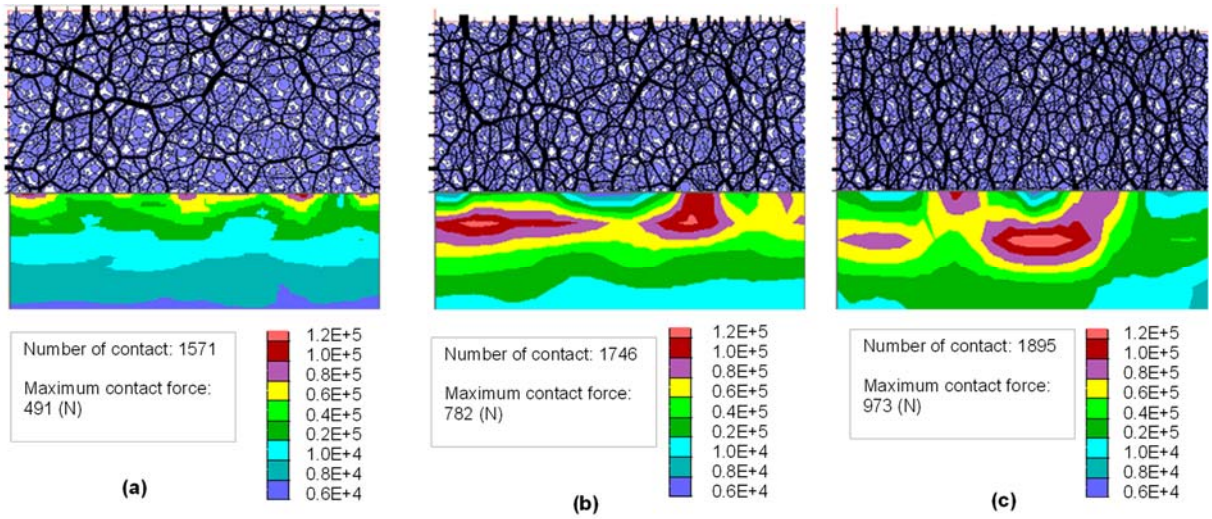

Fig.4. Contact forces and stress contour (σ_{yy}) captured in discrete and continuum zones at different load cycles; (a) 10 cycles; (b) 1000 cycle; and (c) 5000 cycles (modified after Ngo et al. [22])

4.2 Degradation of Ballast Particle

In the current coupled DEM-FEM analysis, the breaks of bonds in a simulated particle approximately represent ballast breakage. Figure 5 illustrates snapshots of the evolution of bond breakage at varying number of cyclic loads under a given load frequency of f=15 Hz. The number and locations of bond breakages at different stages of cyclic loading, varying from 100 cycles to 10,000 cycles are presented in Figures 5a-f. It is seen that, within the first 100 cycles, the majority of the bond breakage happens below the loading plate (i.e. sleepers) due to induced high contact forces, as shown in the Figure 5a. With an increase in cyclic loads there is an increase in the bond breakage (Figures 5b-f) and the re-arrangement of broken bonds (i.e. ballast get compacted and resisted from further degradation), which leads to more contact force distributions in the major principal stress direction as shown in Figures 4b-c. It is seen that the evolution of broken bonds is very similar to the increased ballast breakage observed from the laboratory data [3]. This phenomenon clearly demonstrates that the formation of contact force distributions in the ballast specimens during loading process is dynamic and significantly controlled by the breakage of the grains. Figure 5g illustrates typical locations and re-arrangement of ballast breakage during cyclic loading where bonds are broken and the corresponding particles are separating each other.

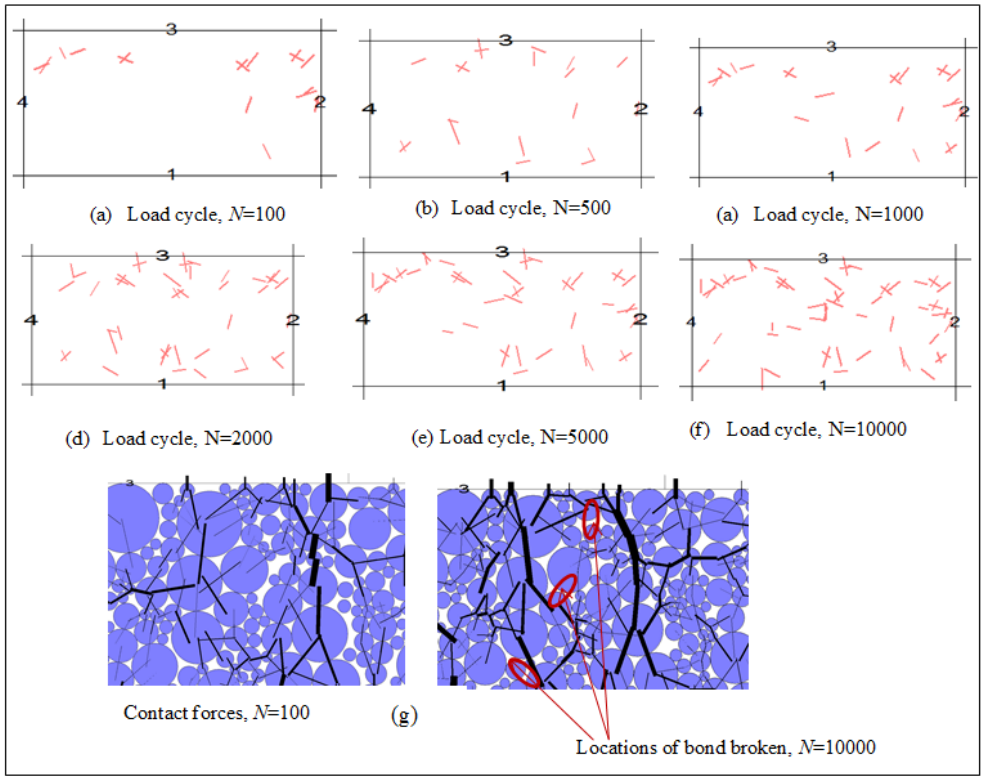

Fig. 5. Snapshots of bond breakage at varying load cycles: *N*=100; (b) *N*=500; (c) *N*=1000; (d) *N*=2000; (e) *N*=5000; (f) *N*=10000

5 Conclusions

A series of large-scale track process simulation apparatus (TPSA) laboratory tests were conducted to investigate the load-deformation responses of railway ballast under cyclic loading. A combined discrete-continuum model was introduced to study load-deformation responses of where the ballast aggregates were modelled by the discrete element method and the subgrade was modelled by finite continuum approach. Subgrade and sub-ballast were modelled using continuum method, having a total thickness of 150 mm to simulate capping formation in the field. Results indicated that the ballast exhibited a significant axial strain at the beginning of loading stage, followed by gradually increasing displacement and then remained relatively unchanged toward the end. Changes of the distribution of contact forces and stress contours induced in the ballast at varying stages of cyclic loading were analysed and it confirmed that the stresses distributed non-uniformly across the ballast assembly where the maximum stresses occurring beneath the sleeper resulting in greater number of broken bond observed. The coupled DEM-FEM model will make an important intellectual contribution to advance knowledge, addressing the interface issues between the discrete and continuum approaches.

6 Acknowledgements

The authors greatly appreciate the financial support from the Rail Manufacturing Cooperative Research Centre (funded jointly by participating rail organisations and the Australian Federal Government's Business Cooperative Research Centres Program) through Project R2.5.1 - Performance of recycled rubber inclusions for improved stability of railways. The authors would like to thank the Australasian Centre for Rail Innovation (ACRI) Limited, and Tyre Stewardship Australia Limited for providing the financial support needed to carry out this research. Some research

outcome is reproduced in this paper with kind permission from the ASCE-International Journal of Geomechanics.The authors are grateful to Mr. Alan Grant, Mr. Cameron Neilson, Mr Duncan Best and Mr. Ritchie McLean for their assistance in the laboratory.

References

1. Indraratna, B., W. Salim, and C. Rujikiatkamjorn, Advanced Rail Geotechnology - Ballasted Track.: CRC Press, Taylor & Francis Group, London, UK (2011).
2. Selig, E.T. and J.M. Waters, Track geotechnology and substructure management.: Thomas Telford, London (1994).
3. Indraratna, B., N.T. Ngo, and C. Rujikiatkamjorn, Deformation of coal fouled ballast stabilized with geogrid under cyclic load. Journal of Geotechnical and Geoenvironmental Engineering, 139(8): p. 1275-1289 (2013).
4. Indraratna, B., N.T. Ngo, and C. Rujikiatkamjorn, Behavior of geogrid-reinforced ballast under various levels of fouling. Geotextiles and Geomembranes,. 29(3): p. 313-322 (2011).
5. Tennakoon, N., B. Indraratna, C. Rujikiatkamjorn, S. Nimbalkar, and T. Neville, The Role of Ballast-Fouling Characteristics on the Drainage Capacity of Rail Substructure. Geotechnical Testing Journal, 35(4): p. 1-11 (2012).
6. Rujikiatkamjorn, C., B. Indraratna, N.T. Ngo, and M. Coop, A laboratory study of railway ballast behavior under various fouling degree. The 5th Asian Regional Conference on Geosynthetics, pp. 507-514, (2012).
7. Tutumluer, E., W. Dombrow, and H. Huang. Laboratory characterization of coal dust fouled ballast behavior. in AREMA 2008 Annual Conference & Exposition. Salt Lake City, UT, USA (2008).
8. Ngo, N.T., B. Indraratna, and C. Rujikiatkamjorn, Micromechanics-based investigation of fouled ballast using large-scale triaxial tests and discrete element modeling. Journal of Geotechnical and Geoenvironmental Engineering, 134(2): p. 04016089, (2017).
9. Lackenby, J., B. Indraratna, G.R. McDowell, and D. Christie, Effect of confining pressure on ballast degradation and deformation under cyclic triaxial loading. Geotechnique, 57(6): p. 527–536 (2007).
10. McDowell, G.R., W.L. Lim, A.C. Collop, R. Armitage, and N.H. Thom, Comparison of ballast index tests for railway trackbeds. Geotechnical Engineering, 157(3): p. 151–161, (2008).
11. Erol, T. and X. Yuanjie, Gradation and Packing Characteristics Affecting Stability of Granular Materials: Aggregate Imaging-Based Discrete Element Modeling Approach. International Journal of Geomechanics, 17(3), (2017).
12. Kaewunruen, S., Remennikov, A. M., ed. Dynamic properties of railway track and its components : a state-of-the-art review. ed. B.e. Weiss. New Research on Acoustics, Hauppauge, New York, Nova Science Publisher. 197-220, (2008).
13. Powrie, W., L.A. Yang, and C.R.I. Clayton, Stress changes in the ground below ballasted railway track during train passage. Proceedings of the Institution of Mechanical Engineers: Part F: Journal of Rail and Rapid Transit, p. 247-261, (2007).
14. Bhandari, A., J. Han, and R.L. Parsons, Discrete Element Method Investigation of Geogrid-Aggregate Interaction under a Cyclic Wheel Load, in Geosynthetics Committee (AFS70). (2008).
15. Ngo, N.T., B. Indraratna, and C. Rujikiatkamjorn, A study of the geogrid–sub-ballast interface via experimental evaluation and discrete element modelling. Granular Matter, 19(3): p. 54, (2017).
16. McDowell, G.R., O. Harireche, H. Konietzky, S.F. Brown, and N.H. Thom, Discrete element modelling of geogrid-reinforced aggregates. Proceedings of the ICE - Geotechnical Engineering 159(1): p. 35-48, (2006).
17. Indraratna, B., S.K.K. Hussaini, and J.S. Vinod, On the shear behavior of of ballast-geosynthetic interfaces. Geotechnical Testing Journal,. 35(2): p. 1-8, (2012).
18. Biabani, M.M. and B. Indraratna, An evaluation of the interface behavior of rail sub-ballast stabilised with geogrids and geomembranes. Geotextiles and Geomembranes, 43(3): p. 240-249,(2015)
19. Indraratna, B., S.S. Nimbalkar, N.T. Ngo, and T. Neville, Performance improvement of rail track substructure using artificial inclusions – Experimental and numerical studies. Transportation Geotechnics, 8: p. 69-85, (2016).
20. Biabani, M.M., B. Indraratna, and N.T. Ngo, Modelling of geocell-reinforced sub-ballast subjected to cyclic loading. Geotextiles and Geomembranes, 2016. 44(4): p. 489-503.
21. AS.289.6.2.2, Methods of testing soils for engineering purposes. Method 6.2.2: Soil strength and consolidation tests—Determination of the shear strength of a soil—Direct shear test using a shear box. 1998: Australian Standard.
22. Ngo, N.T., B. Indraratna, and C. Rujikiatkamjorn, Simulation Ballasted Track Behavior: Numerical Treatment and Field Application. International Journal of Geomechanics, 2017. 17(6): p. 04016130.
23. Indraratna, B., J. Lackenby, and D. Christie, Effect of confining pressure on the degradation of ballast under cyclic loading Geotechnique, 2005. 55(4): p. 325–328.
24. Cundall, P.A. and O.D.L. Strack, A discrete numerical model for granular assemblies. Geotechnique, 1979. 29(1): p. 47-65.
25. Tutumluer, E., H. Huang, and X. Bian, Geogrid-aggregate interlock mechanism investigated through aggregate imaging-based discrete element modeling approach. Int. J. Geomech., 2012: p. 391.

26. Ngo, N.T., B. Indraratna, and C. Rujikiatkamjorn, DEM simulation of the behavior of geogrid stabilised ballast fouled with coal. Computers and Geotechnics, 2014. 55: p. 224-231.
27. McDowell, G.R. and M.D. Bolton, On the micromechanics of crushable aggregates. Geotechnique, 1998. 48(5): p. 667±679.
28. Han, J., A. Bhandari, and F. Wang, DEM analysis of stresses and deformations of geogrid-reinforced embankments over piles. International Journal of geomechanics, ASCE, 2011. 12(4): p. 340-350
29. Itasca, Particle flow code in three dimensions (PFC3D). Itasca Consulting Group, Inc., Minnesota, 2014.
30. Indraratna, B., N.T. Ngo, C. Rujikiatkamjorn, and S.W. Sloan, Coupled discrete element–finite difference method for analysing the load-deformation behavior of a single stone column in soft soil. Computers and Geotechnics, 63: p. 267-278, (2015).
31. Ngo, N., B. Indraratna, C. Rujikiatkamjorn, and M. Biabani, Experimental and discrete element modeling of geocell-stabilized sub-ballast subjected to cyclic loading. J. Geotech. Geoenviron. Eng.,: p. 0401510, (2016)
32. Lobo-Guerrero, S. and L.E. Vallejo, Crushing a weak granular material: experimental numerical analyses. Geotechnique, 55(3): p. 245–249, (2005).
33. Maeda, K., H. Sakai, A. Kondo, T. Yamaguchi, M. Fukuma, and E. Nukudani, Stress-chain based micromechanics of sand with grain shape effect. Granular Matter, 12: p. 499-505, (2010).